APPLIED ORGANOMETALLIC CHEMISTRY
Appl. Organometal. Chem. **13**, 373–382 (1999)

Cracks Developed During $SrTiO_3$ Thin-film Preparation from Polymeric Precursors

S. M. Zanetti,[1]* E. R. Leite,[1] E. Longo[1] and J. A. Varela[2]
[1]Departamento de Química, Universidade Federal de São Carlos, PO Box 676, 13560 São Carlos, SP, Brazil
[2]Instituto de Química, Universidade Estadual Paulista, PO Box 355, 14800 Araraquara, SP, Brazil

Strontium titanate ($SrTiO_3$) thin films were prepared by dip-coating Si(111) single-crystal substrates in citrate solutions of ethylene glycol, considering several citric acid/ethylene glycol (CA/EG) ratios. Measurements of intrinsic viscosity indicate that increasing the amount of EG increases the precursors' polymeric chains and increases the weight loss. After deposition the substrates were dried on a hotplate (≈150 °C); this was followed by heat treatment at temperatures ranging from 500 to 700 °C using heating and cooling rates of 1 °C min^{-1}. SEM and optical microscopy investigations of the sintered films obtained from different CA/EG ratios indicate that there is a critical thickness above which the films present cracks. This critical thickness for $SrTiO_3$ films deposited on the Si(111) substrate is about 150 nm. Measurements of crack spacing as a function of film thickness indicate that the origin of cracks cannot be explained by the elastic behavior of the film but rather by the viscoelastic relaxation of the film during pyrolysis and sintering. Copyright © 1999 John Wiley & Sons, Ltd.

Keywords: sol/gel process; thin films; strontium titanate; cracking; ethylene glycol; citric acid

1 INTRODUCTION

Strontium titanate ($SrTiO_3$) is a material with the perovskite structure that presents useful dielectric properties such as a high dielectric constant, small capacitance temperature coefficient and high volumetric resistivity. These characteristics make this material a suitable candidate to use as thin films, capacitors and dynamic random access memories (DRAMs).[1,2]

$SrTiO_3$ thin films have been prepared by several techniques, such as metallorganic decomposition (MOD),[3] the sol–gel process,[4,5] sputtering[6] and laser ablation.[7] In general these methods lead to crystallization of the $SrTiO_3$ phase with no intermediate phases at temperatures in the range 500–700 °C.

Solution-based methods have been widely used to prepare thin oxide films.[8,9] An advantage of these methods is the ability to control the stoichiometry precisely at the molecular level. The most frequently used solution preparation approaches can be grouped into two categories: (1) sol–gel processes; and (2) metallorganic decomposition.

There are essentially three different kinds of sol–gel process: colloidal sol-gel processes; derivation of inorganic polymeric gels from organometallic compounds, and gel routes involving formation of an organic polymeric glass (polymeric precursor method).

The polymeric precursor method can be divided into two groups.[10] The first is *in situ* polymerization of organometallic monomers and the second involves the preparation of a viscous solution system containing metal ions, polymers and a solvent. This viscous solution can be easily converted to a thermoplastic gel at high polymer concentrations.

The *in situ* polymeric precursors method has been used extensively to obtain ceramic powders with small particle size and single phase.[11,12] This method was originally developed by Pechini[13] and is based on the chelation of a metallic cation by a carboxylic acid, such as citric acid, and further polymerization promoted by the addition of ethylene glycol and consequent polyesterification. However, this method has not been much used to obtain thin films. Liu and Wang[14] reported the deposition of $La_{1-z}Sr_zCo_{1-y}Fe_yO_{3-x}$ on dense or porous substrates using the polymeric precursors method. They obtained nonporous and uniform

* Correspondence to: S. M. Zanetti, Departamento de Química, Universidade Federal de São Carlos, PO Box 676, 13560 São Carlos, SP, Brazil.

 CCC 0268–2605/99/050373–10 $17.50

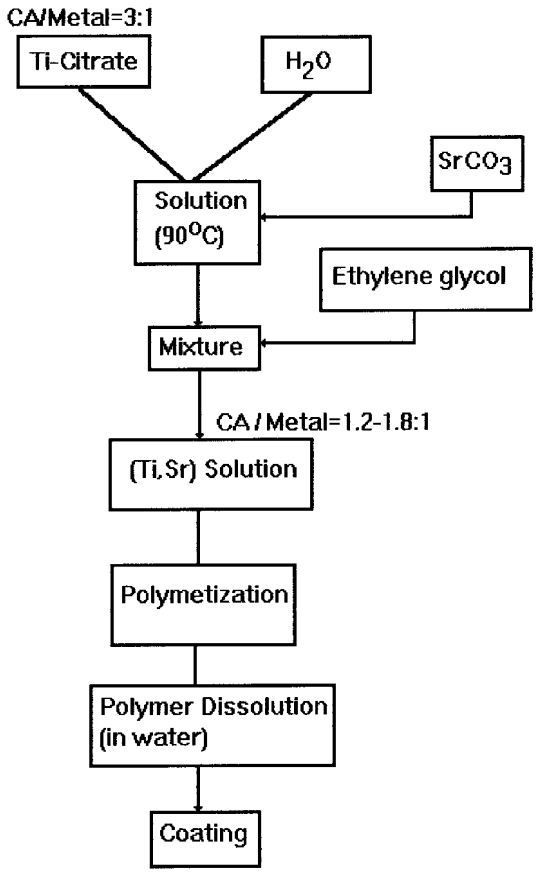

Figure 1 Flow chart for preparaton of $SrTiO_3$ polymeric precursor solution.

crack-free films 400 nm thick with a single dip. The most important parameter in controlling the deposition process, according to Liu and Wang,[14] is the citric acid/metal ratio. They stated that the citric acid/ethylene glycol ratio, on the other hand, is not a critical parameter in obtaining dense and crack-free films.

Olivi *et al.*[15] reported the preparation of SnO_2 thin films with good optical and electrochemical properties by the polymeric precursor method. Recently, Zanetti *et al.*[16] reported the deposition of $SrTiO_3$ thin films on Si(111) substrates prepared by this method. Crack-free films with a smooth surface and dense microstructure were prepared. In this study, no intermediate phase was detected by grazing incident angle X-ray diffraction (GI-XRD) during the crystallization.

An intrinsic problem of the solution-based methods is the large volume change that takes place when the liquid solution transforms into the thin solid inorganic oxide film. This volume change can cause cracking in the film during the pyrolysis and sintering process. Thus, identification of the critical condition for film cracking is very important in obtaining crack-free films by solution-based methods.

The objective of this study was to analyze the effect of the citric acid/ethylene glycol ratio on the polymer structure and on the deposition process of $SrTiO_3$ thin films as well as to identify the critical conditions for obtaining crack-free thin films by *in situ* polymerization.

2 EXPERIMENTAL PROCEDURE

2.1. Synthesis and deposition

Figure 1 shows a flow chart for preparing the $SrTiO_3$ precursor solution. Strontium carbonate (>99%) was dissolved in an aqueous titanium citrate solution prepared from titanium isopropoxide (>99%). The molar ratio of titanium to strontium was 1.00 and the citric acid/metal molar ratio was kept in the range 1.28–1.80. The following citric acid/ethylene glycol mass ratios (CA/EG) were used in this study: 40:60, 50:50 and 60:40. The solutions with several citric acid/ethylene glycol ratios were polymerized at 90 °C for 10 h and solubilized in deionized water (polymeric solution). Films were prepared using 15 mm × 15 mm Si(111) substrates.

Before coating, the Si(111) substrate was cleaned by immersion in a sulfochromic solution, then rinsed several times in deionized water. The viscosity of the polymeric solution was adjusted by adding water to the solution. Dip coating was conducted by immersion of the clean Si(111) substrate in the polymeric solution followed by controlled withdrawal at a speed of 0.33 cm min^{-1} and 0.1 cm min^{-1}. After deposition the substrates were dried on a hotplate (∼150 °C); this was followed by heat treatment at several temperatures for 1 and 2 h, with a heating and cooling rate of 1 °C min^{-1}.

2.2 Characterization

The (Sr, Ti) polymeric precursor, after elimination of water and polymerization, was characterized by simultaneous thermal analysis, TG/DTA (STA 409, Netzsch, Germany) in synthetic air (50 cm^3 min^{-1})

at a constant heating rate of 10 °C min^{-1} from room temperature up to 1200 °C.

The phase evolution was followed by grazing incident X-ray diffraction (GI-XRD) (D 5000, Siemens, Germany), using a grazing incident angle of 2° (θ) and LiF(100) monochromator. The film microstructure was characterized by optical microscopy with polarized light and by scanning electron microscopy (SEM) (DSM 940A, Zeiss, Germany). The film thickness was evaluated using X-ray fluorescence (XRF) (see section 3).

The relative viscosity of the polymer was measured at 24 °C with an Ostwald viscometer.

3 FILM THICKNESS MEASUREMENT BY XRF

One of the factors that modify the X-ray emission characteristics of a material is absorption. Absorption depends directly on the X-ray excited photon path being lower for smaller length paths. For very small paths this factor can be neglected. The following condition can be written:

$$[\mu_p^x \operatorname{cosec}\psi_1' + \mu_s^x \operatorname{cosec}\psi_2']t \ll 1 \qquad [1]$$

where $\mu_p{}^x$ and $\mu_s{}^x$ are the absorption coefficients for primary and secondary radiation, respectively; ψ_1 and ψ_2 are the spectrometer incidence and take-off angles.

The X-ray intensity (I) corresponding to the mass concentration C of a sample can be written as:

$$C = fI \qquad [2]$$

where f is a factor related to the experimental conditions and the equipment used. C is given by:

$$C = \rho V \qquad [3]$$

where ρ is the density and V is the sample volume exposed to the X-ray, Considering that the cylindrical X-ray impinges on an area A of a film with thickness t, the total volume exposed to the X-ray is At.

Hence Equation [3] can be written as:

$$I_x = \rho At.\frac{1}{f} \qquad [4]$$

This means that the intensity is directly proportional to the film thickness t.

Considering Equation [4], and from a calibration curve of X-ray intensity against film thickness obtained from electron microscopy or by ellipsometry, one can determine the film thickness by measuring the intensity of the X-ray leaving the film.

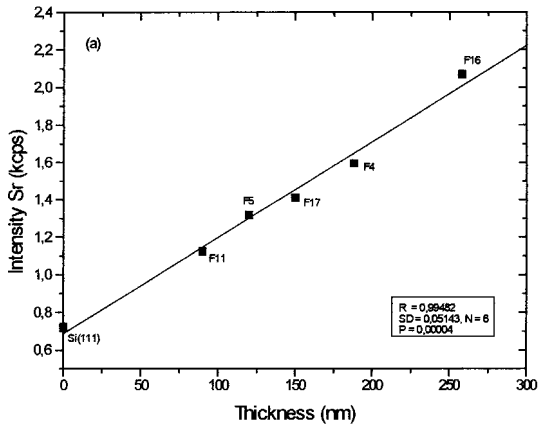

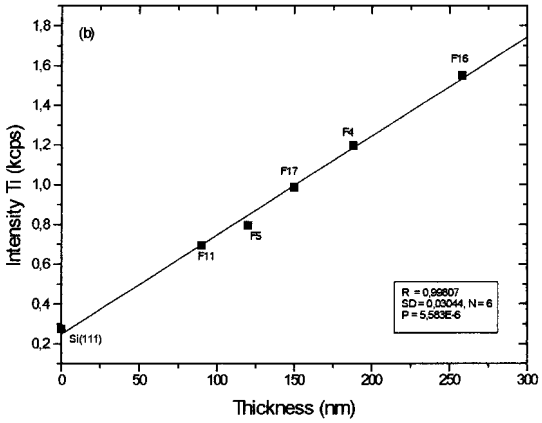

Figure 2 Calibration curves for film thickness obtained by plotting $Sr_{K\alpha}$ and $Ti_{K\alpha}$ X-ray intensities as a function of film thickness measured by SEM.

Figures 2(a) and (b) show the calibration curves for $SrTiO_3$ films deposited on Si(111) substrates, considering the X-ray intensity due to emission of $Sr_{K\alpha}$ and $Ti_{K\alpha}$ respectively, and the thickness measured by SEM. There is a linear relation between the X-ray intensities and the film thickness as predicted by Equation [4].

The empirical equations obtained from the plots of Fig. 2 are:

$$I_{Sr} = 0.685 + 0.0051\,t \qquad [5]$$

$$I_{Ti} = 0.219 + 0.0049\,t \qquad [6]$$

where I_{Sr} and I_{Ti} are the X-ray intensity for Sr and

Table 1. Thickness values obtained from calibration curves and by direct SEM measurements

	Thickness (nm)		
		XRF	
Sample	SEM	Sr	Ti
Si (111)	0	0	0
F4	188	177	190
F5	120	124	110
F11	90	80	90
F16	258	270	261
F17	150	142	148

Ti respectively. The correlation factors for the linear fits of Equations [5] and [6] are greater than 0.99.

Table 1 shows values of different $SrTiO_3$ film thicknesses measured by XRF and by SEM. There is good agreement between the values measured by the two methods.

4 RESULTS AND DISCUSSION

4.1 Experimental results

The effect of the citric acid/ethylene glycol ratio on the molecular weight (M) of the polymeric precursor was estimated by measuring the viscosity and using Equation [7]:

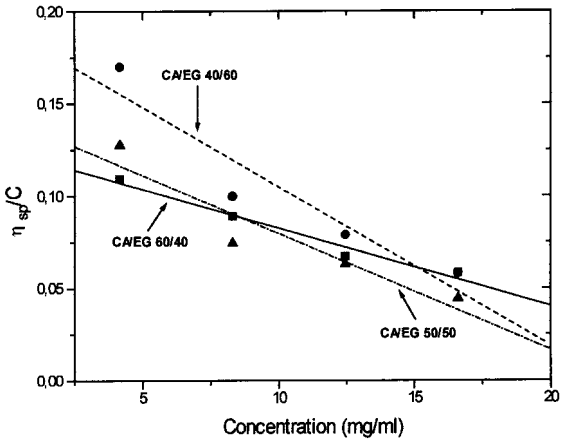

Figure 3 Reduced viscosity (η_{sp}/C) as a function of the concentration of the polymeric precursors in water solution with different ratios of citric acid to ethylene glycol (CA/EG).

Table 2. Intrinsic viscosity [η] of the polymeric precursor with different CA/EG ratios

Polymer (CA/EG ratio)	Intrinsic viscosity [η]
60:40	0.12
50:50	0.13
40:60	0.18

$$[\eta] = KM^{\alpha} \quad [7]$$

where K is a constant that depends on the polymer, solvent and temperature, [η] is the intrinsic viscosity and α is a constant related to the polymer structure. As K and α have not been determined for the $SrTiO_3$ polymeric precursor, they were assumed to be independent of the citric acid/ethylene glycol ratio. Hence the molecular weight was estimated solely by the [η] value.

The intrinsic viscosity [η] was determined from the specific viscosity at different polymeric precursor concentrations according to the Huggins equation [8]

$$\eta_{sp}/C = [\eta] + k[\eta]^2 C \quad [8]$$

where η_{sp} is the specific viscosity, k a constant and C the concentration. η_{sp} was calculated using Equation [9]:

$$\eta_{sp} = \eta_r - 1 \quad [9]$$

where η_r is the relative viscosity.

Figure 3 shows the plot of η_{sp}/C as a function of the concentration of polymeric precursors in the water solution with different ratios of citric acid to ethylene glycol (CA/EG). A linear relationship is observed, as predicted by Equation [8]. The intrinsic viscosity [η] was determined for each CA/EG ratio and the results are listed in Table 2. According to this table, [η] increases with the amount of ethylene glycol. These results suggest that increasing the amount of ethylene glycol promotes an increase in the molecular weight of the polymeric chains of the precursors.

Figure 4 shows the thermogravimetric analysis of the precursors used in this study. Increasing the amount of ethylene glycol leads to more weight loss and consequently a smaller amount of $SrTiO_3$. These results are in accordance with the viscometry data since a precursor with higher molecular weight should have higher weight loss.

Recently, Arina *et al.*[17] reported the formation of a mixed-metal CA complex, with stoichiometry $BaTi(C_6H_6O_7)_3{\cdot}6H_2O$, during the synthesis of $BaTiO_3$ by the polymeric precursor method. In

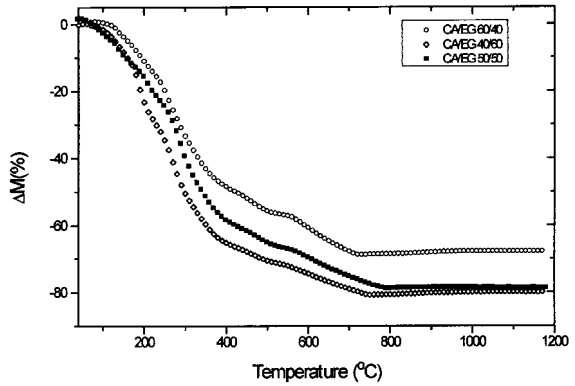

Figure 4 Thermogravimetric analysis of polymeric precursors (heating rate = 10 °C min^{-1}).

the formation of a mixed-metal CA complex, with empirical formula $SrTi(C_6H_6O_7)_3{\cdot}xH_2O$, during the chelation process of Sr^{2+} and Ti^{4+}, there are at least six (COO^-) free groups. These free carboxylic-acid groups may react with EG forming the polymeric chains by a polyesterification reaction. With the increase in EG concentration, more ester groups are formed, leading to an increase in the polymer precursor molecular weight.

Figure 5 shows the variation in thickness of the $SrTiO_3$ thin film (heat-treated at different temperatures, −500°C to 700°C) as a function of the relative viscosity of the polymeric solutions, for films prepared by dip coating with a withdrawal speed of 0.33 cm min^{-1}. As observed in Fig. 5, the films processed from solution with a CA/EG ratio of 60:40 always contained cracks. The films processed from solution with a CA/EG ratio of 40:60 appeared crack-free whereas the films processed from solution with a CA/EG ratio of 50:50 presented cracks for thicker films (films of thickness 180–200 nm). Experimental results indicate the existence of a critical thickness for obtaining crack-free films. For the $SrTiO_3$ film processed by the polymeric precursor method and deposited on the Si(111) single crystal, this critical thickness is approximately 150 nm. Intrinsic parameters of the polymeric precursor such as molecular weight directly affect the film thickness. To maintain the same deposition viscosity for all solutions, it is necessary to increase the polymer concentration of solutions from precursors with lower molecular weight. Since these precursors have a higher concentration of chelated cations, increasing the concentration leads to an increase in the amount of deposited $SrTiO_3$ and consequently

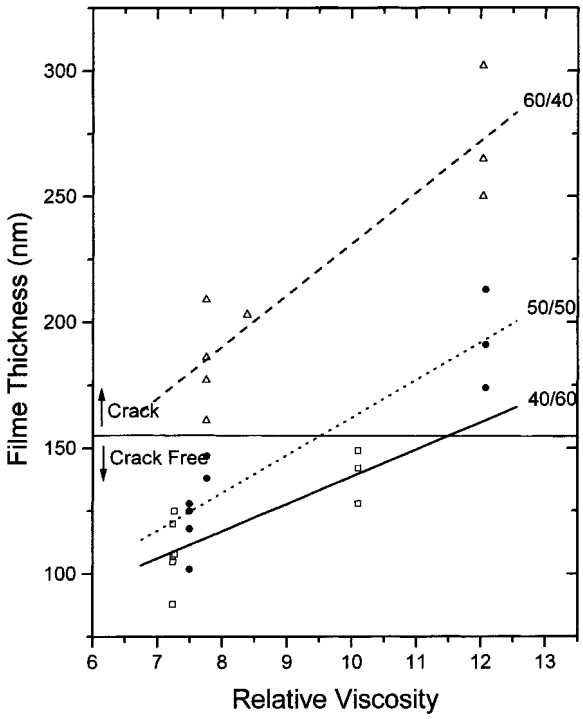

Figure 5 $SrTiO_3$ film thickness as function of relative viscosity of solutions of polymeric precursors with different CA/EG ratios.

in film thickness. Films prepared from the CA/EG 60:40 solution were always thicker than 150 nm in the relative viscosity range used in this study. Decreasing the relative viscosity or varying the deposition velocity makes it possible to obtain

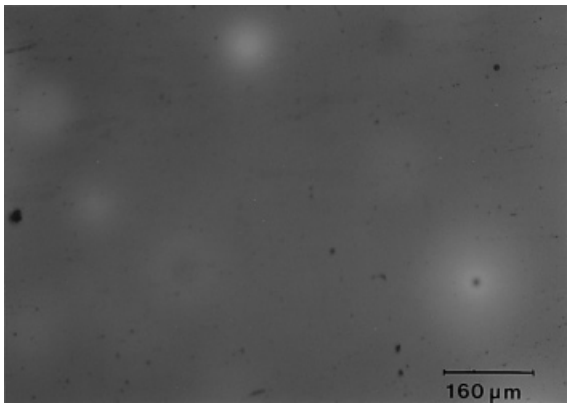

Figure 6 Optical micrograph of film obtained from CA/EG 60:40 solution (relative viscosity = 7.8, withdrawal speed = 0.1 cm min^{-1}).

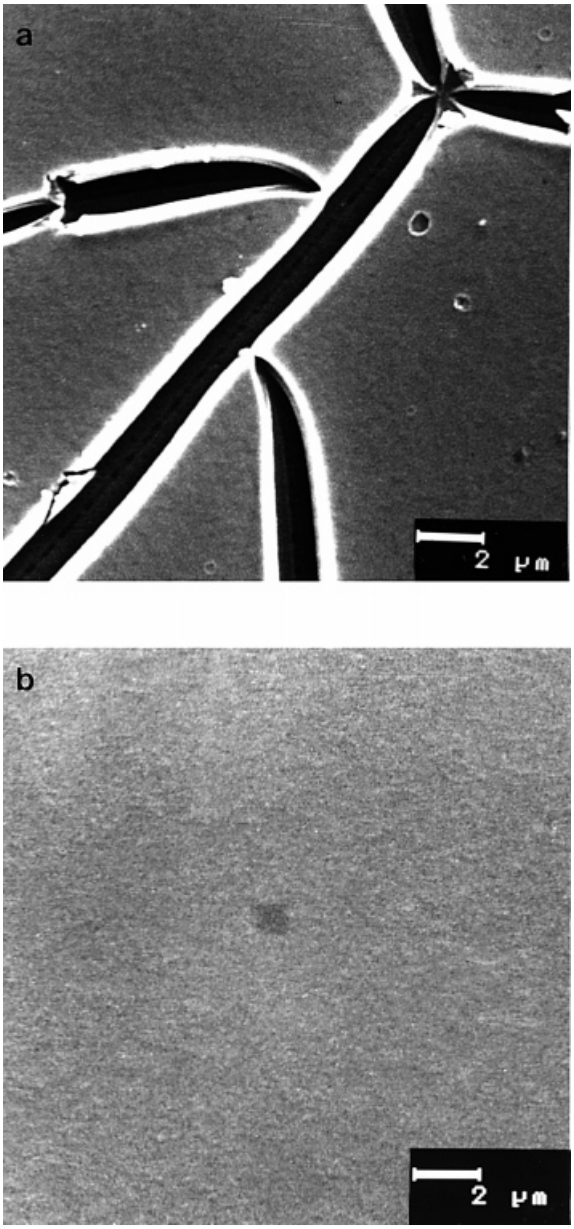

Figure 7 SEM of films obtained from (a) CA/EG 60:40 solution; (b) CA/EG 60:60 solution.

crack-free films using precursors with a CA/EG ratio of 60:40.

Figure 6 shows the micrograph of the $SrTiO_3$ film prepared from the precursor solution with a CA/EG ratio of 60:40, and a relative viscosity of 7.8, obtained with a withdrawal speed of 0.1 cm min^{-1} and calcined at 650 °C for 1 h. The film obtained is crack-free with a thickness of 132 nm.

The micrograph of Figure 7 shows films obtained from precursor solutions with CA/EG ratios of 60:40 and 40:60, heat-treated at 750 °C for 2h. The results of GI-XRD analysis for the sintered films show the formation of a single $SrTiO_3$ phase. A crack-free surface (Fig. 7b) is observed in the film obtained from solution with a CA/EG ratio of 40:60, whereas the film obtained from the solution with a CA/EG ratio of 60:40 shows straight and long cracks (Figure 7a) similar to those observed by Chen and Chen[18] for $BaTiO_3$ and PZT ($PbZr_xTi_{1-x}O_3$) films. According to those authors, this type of crack is caused by external factors such as dust particles; in this case, films were not prepared in a clean room.

Figure 8 shows a set of optical micrographs in which small particles are visible on the film surface. Figure 8(a) shows the $SrTiO_3$ film prepared from a precursor with a 40:60 CA/EG ratio, sintered at 550 °C for 1 h. The presence of particles on the film did not promote cracks (film thickness 107 nm). Figure 8(b) presents the film prepared from a precursor with a 50:50 CA/EG ratio, heat-treated in the same conditions. Small cracks are observed near the particles. However, these cracks did not propagate (film thickness 125 nm). Finally, Figure 8(c) shows the micrograph of the film prepared from the precursor with CA/EG ratio of 60:40. Large straight cracks are observed (film thickness 213 nm). These results are in agreement with the assumption that a critical thickness exists for obtaining crack-free films.

4.2 General discussion

Thermal analysis and viscometry results show that the CA/EG ratio controls the molecular weight of the precursor polymeric chains, as well as the amount of chelated cations. The main role of the CA/EG ratio is to control the viscosity of the polymeric precursor solution for deposition. For each ratio there is an optimum viscosity at which films thinner than the critical thickness are obtained, avoiding crack formation. Although no direct relationship has been reported for the CA/EG ratio and crack formation, this ratio is fundamental in controlling the thickness of the deposited film, although Liu and Wang[14] assumed that it was not important in the film deposition process.

The experimental results indicate the existence of a critical thickness at which crack propagation starts. These results are in agreement with those

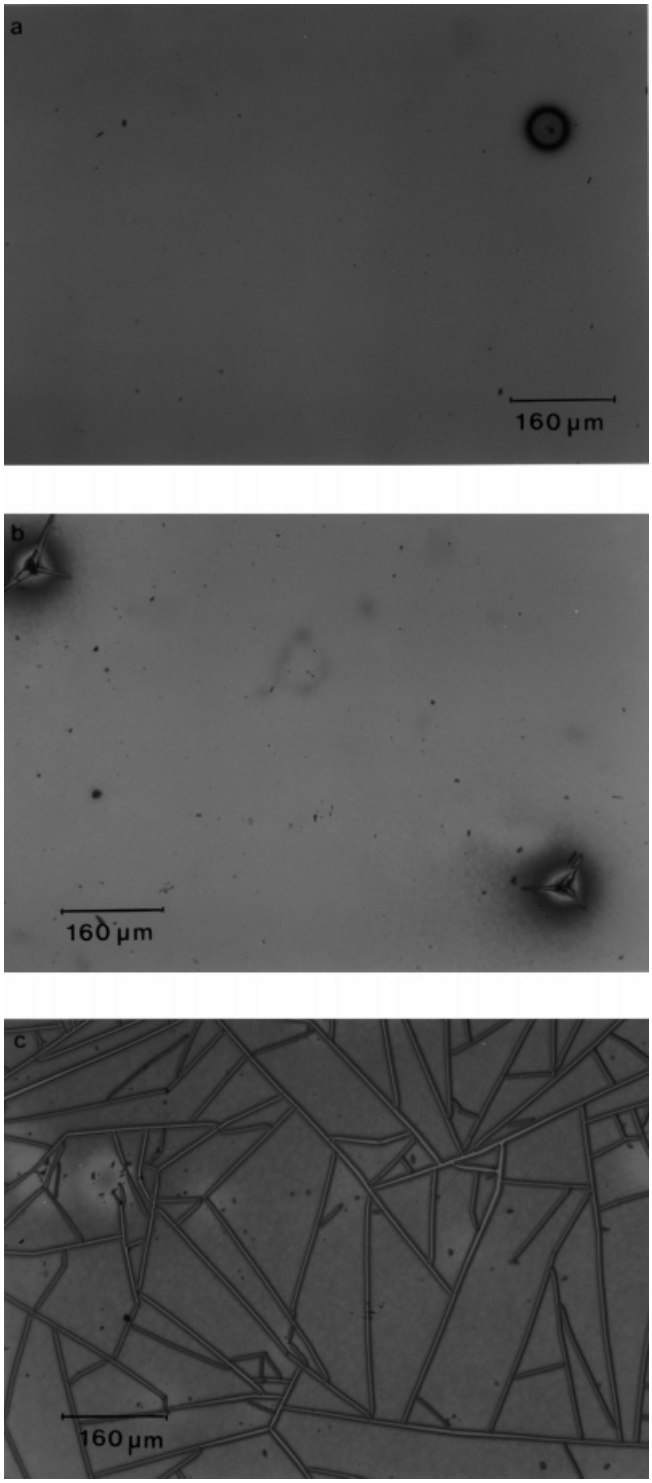

Figure 8 Films prepared from (a) CA/EG 40:60 precursor (film thickness = 107 nm); (b) CA/EG 50:50 precursor (film thickness = 125 nm); (c) CA/EG 60:40 precursor (film thickness = 213 nm).

reported in the literature for different film compositions obtained by chemical or physical methods.[18,19]

Thouless[20] suggested that the mean crack spacing (λ) propagated in thin films deposited on an elastic substrate is related to the stress intensity factor (K_{IC}), film thickness (t) and stress (σ) according to Equation [10]:

$$\lambda \cong 5.63\sqrt{t}\frac{K_{IC}}{\sigma} \qquad [10]$$

In this model the critical film thickness (t_c) is given by:

$$t_c = 0.50\left(\frac{K_{IC}}{\sigma}\right)^2 \qquad [11]$$

Considering that the experimentally determined critical thickness for the $SrTiO_3$ film is 150 nm, K_{IC}/σ can be estimated and used to calculate λ. Figure 9 shows the variation of λ as a function of t calculated using Equation [10]. The predicted value is 10 to 20 times smaller than experimentally measured. Note also, in Fig. 9, that λ increases with t up to $t = 210$ nm, before decreasing.

Figure 10 shows a set of SEM micrographs obtained of films with different crack sizes. An increase in crack spacing is observed (Fig. 10a,b,c) for films with thickness between 178 and 203 nm, as well as an increase in crack width with film thickness. Atkinson and Guppy[21] also reported this tendency. For thicker films λ decreases due to additional crack formation within crack-free regions (Figure 10d).

The significantly larger value found for λ, as well as the crack thickness increase with film thickness, indicates that interfacial delamination, shear strain at the film–substrate interface and/or viscoelastic relaxation of the film might occur in addition to elastic relaxation. Among these factors the viscoelastic relaxation of the film is the likely origin of stresses causing crack formation.[18,21] These stresses are developed during pyrolysis of the organic material precursor and the subsequent sintering process.

Analysis of the results suggests that the origin of the cracks developed in films prepared from the polymeric precursor method is similar to those described by Chen and Chen[18] for films processed by MOD. Atkinson and Guppy[21] also suggest the dominance of viscoelastic relaxation as the origin for stresses that promote cracks in CeO_2 films prepared by the sol–gel method.

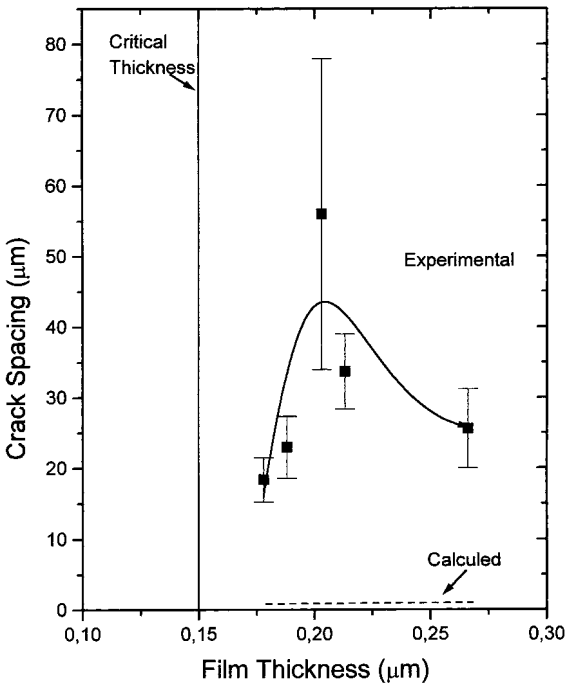

Figure 9 Crack spacing (λ) as function of film thickness (t).

5 CONCLUSIONS

The results of this study lead to the following conclusions for films prepared from polymeric precursor solutions:

(a) The CA/EG ratio greatly affects the molecular weight of polymeric chains as well as the amount of chelated cations.
(b) The experimental results indicate the existence of a critical thickness for obtaining crack-free films. For $SrTiO_3$ deposited on Si(111) substrate this thickness is approximately 150 nm.
(c) Crack formation is probably caused by viscoelastic relaxation during the processes of pyrolysis and sintering of the thin film.

Acknowledgements The authors acknowledge Professor Seshu B. Desu and Dr Carlos T. A. Suchicital of the Virginia Polytechnique Institute for discussions and donation of silicon substrates. The following Brazilian financing support agencies are acknowledged: FAPESP, CNPq, CAPES and FUNDAÇÃO BANCO DO BRASIL.

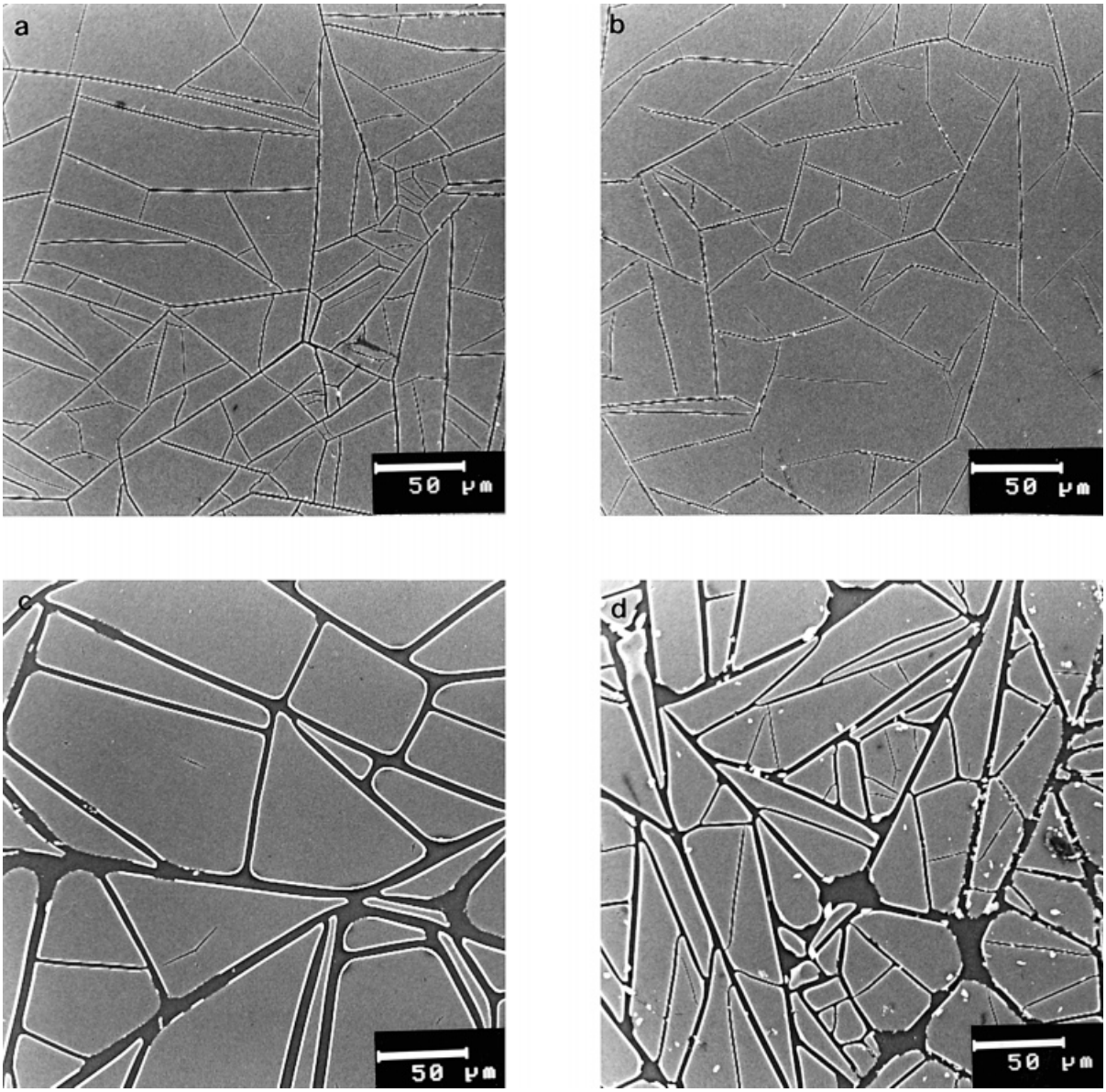

Figure 10 SEM of films with different crack sizes. Film thickness: (a) 178 nm; (b) 183 nm; (c) 203 nm, (d) 266 nm.

REFERENCES

1. M. Iwabachi, and T. Kobayashi, *J. Appl. Phys.* **75**, 5245 (1994).
2. U. Syamaprassad, P. K. Galgali, and B. L. Mohanty, *Mater. Lett.* **7**, 197 (1988).
3. P. C. Joshi, and S. B. Krupanidhi, *J. Appl. Phys.* **73**, 7627 (1993).
4. D. M. Tahan, A. Safari, and L. C. Klein, *J. Am. Ceram. Soc.* **79**, 1593 (1996).
5. U. Selvaraj, A. V. Prasadarao, S. Komarneni, and R. Roy, *Mater. Lett.* **23**, 123 (1995).
6. T. Horikawa, N. Mikami, T. Makita, J. Tanimura, M. Kataoka, K. Sato, and M. Nunoshita, *Jpn. J. Appl. Phys.* **32**, 4126 (1993).

7. S. B. Krupanidhi, and G. M. Rao, *Thin Solid Films* **240**, 1593 (1994).
8. J. M. Thomas, Optical coating fabrication. In: *Sol–Gel Optics: Processing and Applications*, Klein, L. C. (ed), Kluwer, Boston, 1994, p. 141.
9. D. S. Hagberg, and D. A. Payne, Nonsilicate optical coatings. In: *Sol–Gel Optics: Processing and Applications*, Klein, L. C. (ed), Kluwer, Boston, 1994, p. 169.
10. M. Kakihama, *J. Sol–Gel Sci. Technol.* **6**, 7 (1996).
11. E. R. Leite, C. M. G. Souza, E. Longo, and J. A. Varela, *Ceram. Int.* **21**, 143 (1995).
12. M. Cerqueira, R. S. Nasar, E. Longo, E. R. Leite, and J. A. Varela, *Mater. Lett.* **22**, 181 (1995).
13. M. P. Pechini, US Patent 3 330 697 (1967).
14. M. Liu, and D. Wang, *J. Mater. Res.* **10**, 3210 (1995).
15. P. Olivi, E. C. Pereira, E. Longo, J. A. Varela, and L. O. S. Bulhões, *J. Electrochem. Soc.* **140**, L81 (1993).
16. S. M. Zanetti, E. Longo, J. A. Varela, and E. R. Leite, *Mater. Lett.* **31**, 173 (1997).
17. M. Arima, M. Kakihama, Y. Nakamura, M. Yashima, and M. Yoshimura, *J. Am. Ceram. Soc.* **79**, 2047 (1996).
18. S. Y. Chen, and I. W. Chen, *J. Am. Ceram. Soc.* **78**, 2929 (1995).
19. E. Olsson, A. Gupta, M. D. Thouless, and A. Segmuller, *Appl. Phys. Lett.* **58**, 1682 (1991).
20. M. D. Thouless, *J. Am. Ceram. Soc.* **73**, 2144 (1990).
21. A. Atkinson, and R. M. Guppy, *J. Mater. Sci.* **126**, 3869 (1991).

